International Journal of Marine Engineering Innovation and Research, Vol. 8(2), Jun. 2023. 310-323
(pISSN: 2541-5972, eISSN: 2548-1479)

Fatigue Life Analysis of FSO Anchor Chain with Corrosion Effect

Dewinta Putri Cahyaningtyas[1], Nur Syahroni[2], Rudi Walujo Prastianto[3], Eko Budi Djatmiko[4], Murdjito[5], Hafizh Muhammad Naufal Shidqi[6]

(Received: 01 June 2023 / Revised: 06 June 2023 /Accepted: 06 June 2023)

***Abstract*— In this study, the authors analyze the fatigue life of the anchor chain used to secure the Gamkonora FSO to the seabed. The objective is to determine the operational lifespan of the anchor chain by considering its fatigue life. The research begins with an analysis of the movement of the Gamkonora FSO under environmental loads in both free-floating and moored conditions to determine the tension in each anchor chain. Next, the anchor chain tension is calculated for various corrosion levels, namely 0%, 5%, 10% and 15%. Subsequently, the tension range and damage ratio values are determined using the T-N curve method based on Palmgren Miner's failure law, with failure estimation carried out using the rainflow counting method. The numerical modeling results reveal that the largest translational motion behavior of the FSO occurs during heave motion, reaching 1.409 m/m, while the largest rotational motion is observed during roll motion, with a value of 3.463 deg/m when the FSO is fully loaded. The maximum tension recorded in the anchor chain is 1,695.14 kN at heading 90° under 0% corrosion conditions, with a safety factor of 4.53. Furthermore, the cumulative damage value from the T-N curve is obtained, with the largest value recorded as 0.0702. Based on the cumulative damage, the fatigue life of the anchor chain is estimated to be 14.25 years during its operational lifespan.**

Keywords—Cumulative Damage, Damage Ratio, Failure, Rainflow Counting, Tension Range, T-N Curve.

I. INTRODUCTION

An offshore structure can be defined as a structure that is detached directly from the land, whether it is a fixed or floating structure. With the advancements in offshore oil and gas drilling technology, there has been a growing trend towards using floating structures for exploration and exploitation. A floating structure is a type of offshore building that is designed to float in the open sea, allowing it to move with the waves. Its key characteristics are mobility and the ability to anticipate movement caused by waves, wind, and currents. Generally, this type of building is allowed to move freely within six degrees of freedom (surge, sway, heave, roll, pitch, and yaw) [1].

A Floating Storage and Offloading (FSO) facility is a floating structure operating in an offshore oil and gas field. Its purpose is to receive, store, and distribute crude oil. The FSO structure receives crude oil through an offloading line for transportation to a designated site. It typically consists of a large ship-like structure, which can be either a newly constructed vessel or a modified tanker, that is permanently moored at its operational location.

The mechanism of the mooring system in maintaining the position of the structure is to withstand the global forces that occur on the structure [2]. The mooring system itself has various configurations that can be used such as single point mooring, spread mooring, turret mooring, and others which will be selected according to the environmental conditions in the area [3]. This study focuses on the mooring spread at the FSO Gamkonora. The research was conducted in response to cases of undersea pipeline leaks that occurred at PAPA Terminal.

According to [4], operational floating marine structures require mooring equipment. The mooring system is necessary to prevent the structure from moving or shifting away from its designated work location. Additionally, the system is expected to withstand environmental loads such as wave loads, wind loads, and current loads. The mooring system utilized in this study is called spread mooring, which involves multiple mooring legs spread across the bow and stern.

According to [5], the phenomenon of damage or reduced structural strength due to loads, especially cyclic loads, is known as structural fatigue (fatigue), and is essentially characterized by cracks and in the subsequent process propagation and damage occur (failure). Malfunctions in the mooring line system are often caused by fatigue in the anchor chain, both in its construction and the structure itself. Fatigue remains the primary cause of damage to marine structures. Fatigue is influenced by cyclic loads continuously experienced by the construction and structure during operation. Estimating fatigue life is done based on the load fluctuations that the structure will

Dewinta Putri C, Department of Ocean Engineering, Institut Teknologi Sepuluh Nopember, Surabaya, 60111, Indonesia E-mail : dewinta.putri7@gmail.com
Nur Syahroni, Department of Ocean Engineering, Institut Teknologi Sepuluh Nopember, Surabaya, 60111, Indonesia E-mail : nsyahroni@oe.its.ac.id
Rudi Walujo P, Department of Ocean Engineering, Institut Teknologi Sepuluh Nopember, Surabaya, 60111, Indonesia E-mail : rudiwp@oe.its.ac.id
Eko Budi D, Department of Ocean Engineering, Institut Teknologi Sepuluh Nopember, Surabaya, 60111, Indonesia. E-mail : ebdjatmiko@oe.its.ac.id
Murdjito, Department of Ocean Engineering, Institut Teknologi Sepuluh Nopember, Surabaya, 60111, Indonesia. E-mail : murdjito@oe.its.ac.id
Hafizh M Naufal S, Department of Ocean Engineering, Institut Teknologi Sepuluh Nopember, Surabaya, 60111, Indonesia. E-mail : hafizhnaufal15@gmail.com

experience throughout its operating life. Wave loads predominantly contribute to the loads endured by marine structures, making them more prone to fatigue. Additionally, operational factors at specific levels further increase the cyclic load and thus exacerbate the structural vulnerability [6].

The anchor chain directly experiences fatigue due to both static and dynamic cyclic loads. Generally, the load on the anchor chain construction originates from the spread mooring chain, as well as dynamic loads resulting from operational cyclic loads from the spread mooring, such as wave and wind loads, and current loads acting on the anchor chain. Consequently, the chain construction becomes susceptible to fatigue due to these loads.

Wu et al. (2014) [7] identified the most critical fatigue damage locations for different mooring systems. The factors affecting the critical location, such as mooring pattern, pretensions, chain length, water depth are discussed, thus provides recommendations for mooring fatigue design of offshore structures.

Kang et al. (2016) [8] studied fatigue analysis of spread mooring line. Contribution of environmental loads (wind, wave, current), type of responses (Wave Frequency and Low-Frequency motions), vessel offsets, mooring position, loading conditions (ballast, intermediate, full) and riser behavior (with and without riser) are investigated.

Given this background, this research aims to analyze the fatigue life of the mooring chain at Gamkonora FSO, which is moored using spread mooring and operates at the PAPA Terminal. In this case, the anchor chain requires a fatigue life analysis to determine whether it is still suitable for operation or not.

II. METHOD

A. Study of Literature

Currently, the activities in this research involve studying literature related to the research. The literature focuses on two main areas: the analysis of mooring rope tension in floating structures and the fatigue life of floating structures. These topics are explored through the use of numerical methods or software assistance. Additionally, the literature covers various aspects such as time domain analysis, anchor chain properties, wave analysis, and relevant rules and codes pertaining to mooring systems.

B. Data Collection

During this stage, data has been collected from FSO Gamkonora, including hydrostatic data and mooring line properties. Additionally, environmental data related to the FSO Gamkonora project has been obtained.

C. FSO Modeling

In this research, the modeling of the Gamkonora FSO structure was conducted using Vessel modeling software. This software not only assists in creating a model of the structure but also enables the analysis of its motion behavior under free floating conditions. By utilizing Vessel modeling software, researchers were able to simulate and understand the dynamic characteristics and response of the Gamkonora FSO structure when it is floating freely. To keep floating structure stable at predetermined boundaries a well-structured mooring system is needed. From a variety of mooring system configurations, mooring links are considered suitable for floating structure [9].

D. FSO Hydrostatic Validation

To ensure the accuracy of the modeling, the hydrostatic data obtained from Vessel modeling software for the FSO Gamkonora is validated against the existing hydrostatic data. The purpose of this validation is to determine the error rate in the modeling process. In this case, the error rate is evaluated according to (IACS) guidelines [10] which are shown ini the table 1. While the validation of the FSO and export tanker structure modeling refers to the 2018 ABS, where the error of the hydrostatic data parameters must be below 2% [11]. By comparing the hydrostatic data from the Vessel modeling software with the existing data, researchers can assess the level of agreement and identify any discrepancies or errors in the modeling process. This validation step is crucial in ensuring the reliability and validity of the hydrostatic data used in the research.

TABLE 1.
MODEL VALIDATION CRITERIA

Hull Form Dependent	
Displacement	+/- 2%
Longitudinal center of buoyancy, from AP	+/- 1% / 50 cm
Vertical center of buoyancy	+/- 1% / 5 cm
Transverse center of buoyancy	+/- 0.5% of B / 5 cm
Longitudinal center of flotation, from AP	+/- 1% / 50 cm
Moment to trim 1 cm	+/- 2%
Transverse metacentric height	+/- 1% / 5 cm
Longitudinal metacentric height	+/- 1% / 50 cm
Cross curves of stability	+/- 5 cm

E. RAO FSO Analysis Free Floating Condition

RAO contains information about the characteristics of the movement of marine structures presented in graphical form, where the abscissa is the frequency parameter, while the ordinate is the ratio between the amplitude of the movement in a certain mode, ζk0, and the wave amplitude, ζ0. The RAO equation [12] can be found by the formula:

$$RAO(\omega) = \frac{\zeta_{k0}(\omega)}{\zeta_0(\omega)} \quad (1)$$

$\zeta_{k0}(\omega)$ = structure amplitude (m)
$\zeta_0(\omega)$ = wave amplitude (m)

Analyzing the motion response of the Gamkonora FSO structure to understand its movement characteristics in a free floating condition. This analysis aims to examine how the structure responds to environmental forces such as waves, wind, and currents.

By conducting this analysis, researchers can obtain the Response Amplitude Operator (RAO) data for each structure. RAO data provides information about the amplitude and phase of the structural response at various frequencies. These data points are crucial for understanding the dynamic behavior of the structure and can be utilized in subsequent steps of the research.

Analyzing the motion response and obtaining RAO data allows researchers to gain insights into how the Gamkonora FSO structure behaves under different environmental conditions. This information is valuable for assessing the structural integrity, stability, and safety of the FSO in real-world scenarios.

Once vessel and its mooring system have been modeled, the static analysis was performed to compute the equilibrium position of the moored structure. Then, dynamic analysis using a time domain approach was performed. This analysis intended to obtain moored structure offset and mooring lines forces [13].

F. Anchor Chain Tension Analysis

In this stage of the research, the stress analysis of the Anchor Chain is conducted using Dynamic analysis software. This analysis considers multiple load cases based on input data from FSO Gamkonora, mooring data, and environmental data. The goal is to assess the stress levels in the Anchor Chain under various load conditions.

The analysis begins by calculating the loads that impact the Anchor Chain for each load case, considering factors such as wave loads, wind loads, and other relevant loads. Once the loads are determined, a stress analysis is performed for each load case. This analysis helps identify the loading combinations that contribute to the stress experienced by the Anchor Chain.

For the analysis, a time domain-based approach is adopted, following the guidelines. The time domain analysis method offers more precise modeling of non-linear factors, including system matrices and external loads. However, it does require a longer calculation time compared to the frequency domain analysis. According to [14], a minimum time domain simulation of 3 hours is recommended.

The maximum tension is the mean tension plus the combined wave frequency and low frequency tension. Determining the value of the maximum tension can be done with the following formula [15]:

$$\boldsymbol{T_{max} = T_{mean} + T_{lfmax} + T_{wfsig}} \quad (2)$$

$$\boldsymbol{T_{max} = T_{mean} + T_{wfmax} + T_{lfsig}} \quad (3)$$

Where:

Tmax = *maximum tension*
Tmean = *mean tension*
Twfmax = *maximum wave frequency tension*
Twfsig = *significant wave frequency tension*
Tlfmax = *low wave frequency tension*
Twfsig = *significant low frequency tension*

The maximum value is used to see the largest response that occurs. The significant value is used to give the dominant value of the tension that occurs [16]. This is important considering that the mooring line functions as structural support due to the influence of external loads. In the simulation, time-domain analysis is used which can produce linear or non-linear values from the response of the mooring line due to the movement of the structure [17].

G. Corroded Anchor Chain Tension Analysis

Analyzing the stress that occurs in the anchor chain which is corroded according to many load cases using Dynamic analysis software based on the results of the anchor chain stress analysis which has been calculated in advance the effect of the combination of loads. The estimated corrosion rate per year is set in the [18] which is shown in table 2 below.

TABLE 2.
CHAIN CORROSION AND WEAR ALLOWANCE [18]

Chain Location	*Corrosion and Wear allowance on Criteria Diameter (mm/year)*[5]	
	Low DIN Level[3]	*High DIN Level*[4]
Splash Zone[1]	0.2 ~ 0.4	0.8
Mid-catenary[2]	0.1 ~ 0.2	0.3
Touch down zone	0.2 ~ 0.4	0.4

Note:
1. *Splash zone: the chain links that are periodically in and out of the water when the unit is at its operating depth. In general, this zone is between 5 m above and 4 m below the waterline.*
2. *Mid-catenary: mooring line below the splash zone and always above the touch down point.*
3. *DIN level smaller than 1 mgN/L*
4. *DIN level close to 7 mgN/L, such as in West Africa*
5. *Higher corrosion allowance should be considered if pitting corrosion associated with Microbiologically Influenced Corrosion (MIC) is suspected*

H. Rainflow Counting

The rainflow counting method is a method used to calculate the voltage range cycles. The stress range and cycle data can then be used to determine the fatigue life of a structure. This method is likened to water falling from a pagoda roof and falling onto another pagoda roof below. The following is an overview of the rainflow counting method [19] which can be seen in Figure 1.

The rainflow counting method involves identifying and analyzing the stress range and cycle data in a structure. It captures the varying stress levels experienced by the structure over time, accounting for both the high and low stress points. By extracting these stress range cycles, the method enables the determination of the fatigue life of the structure.

The concept of rainflow counting helps to identify the repeating stress cycles within the structural loading history, allowing for accurate fatigue life estimation. It provides a systematic approach to capture the stress fluctuations that occur during the operation of a structure.

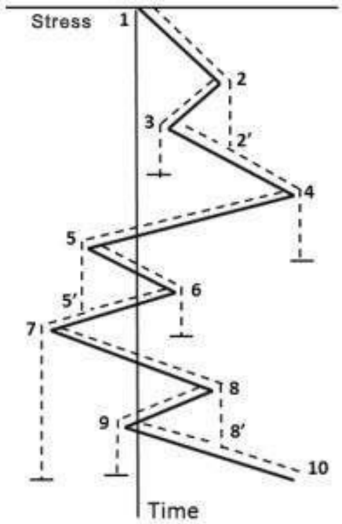

Figure 1. Rainflow Counting Method

I. Fatigue Analysis

The analysis was carried out using the Dynamic analysis software, the results of running the Dynamic analysis software produce tension values for each load case. Furthermore, the calculation of the cumulative estimate of fatigue failure is performed to obtain the value of fatigue damage [15].

$$NR^M = K \quad (4)$$

where

N = Number of cycles

R = Ratio of voltage range (double amplitude) to reference breaking strength (RBS).

J. Fatigue Life Analysis

In the analysis of fatigue life for the anchor chain, the results obtained from the anchor chain fatigue damage are utilized. The fatigue damage is assessed based on the T-N curve, which follows Palmgren Miner's failure law [15].

The T-N curve represents the relationship between the number of stress cycles (N) and the corresponding fatigue life (T) for a given material or component. It helps in estimating the remaining fatigue life of the anchor chain based on the accumulated damage.

Palmgren Miner's failure law states that fatigue failure occurs when the cumulative damage exceeds a certain threshold. The law assumes that each stress cycle contributes to the cumulative damage, regardless of the stress magnitude. By comparing the cumulative damage with the fatigue strength of the material, the remaining fatigue life of the anchor chain can be determined.

By utilizing the T-N curve and Palmgren Miner's failure law, researchers can evaluate the fatigue life of the anchor chain. This information aids in understanding the expected durability of the chain and can guide maintenance and replacement decisions to ensure the safe operation of the FSO Gamkonora.

$$N_f = \frac{1}{D}\,(years) \ldots\ldots\ldots\ldots\ldots\ldots\ldots\ldots\ldots\ldots\ldots\ldots (5)$$

Where,

$N_f = Fatigue\ Life$

III. RESULTS AND DISCUSSION

A. FSO Modeling

FSO Gamkonora is one of the assets owned by DKPU ITS [20]. Gamkonora FSO modeling using Vessel modeling software with principal dimension data and General Arrangement as follows in table 3 and Figure 2:

TABLE 3.
PRINCIPAL DIMENSION DATA FSO GAMKONORA

NO	Principal Dimension	Unit	Dimension
1	Length overall (LOA)	m	244.5
2	Length between perpendicular (LPP)	m	233
3	Breadth (B)	m	44
4	Depth (H)	m	21.5
5	Draft (T)	m	12.7
6	DWT	ton	88,258
7	Displacement	ton	109,431

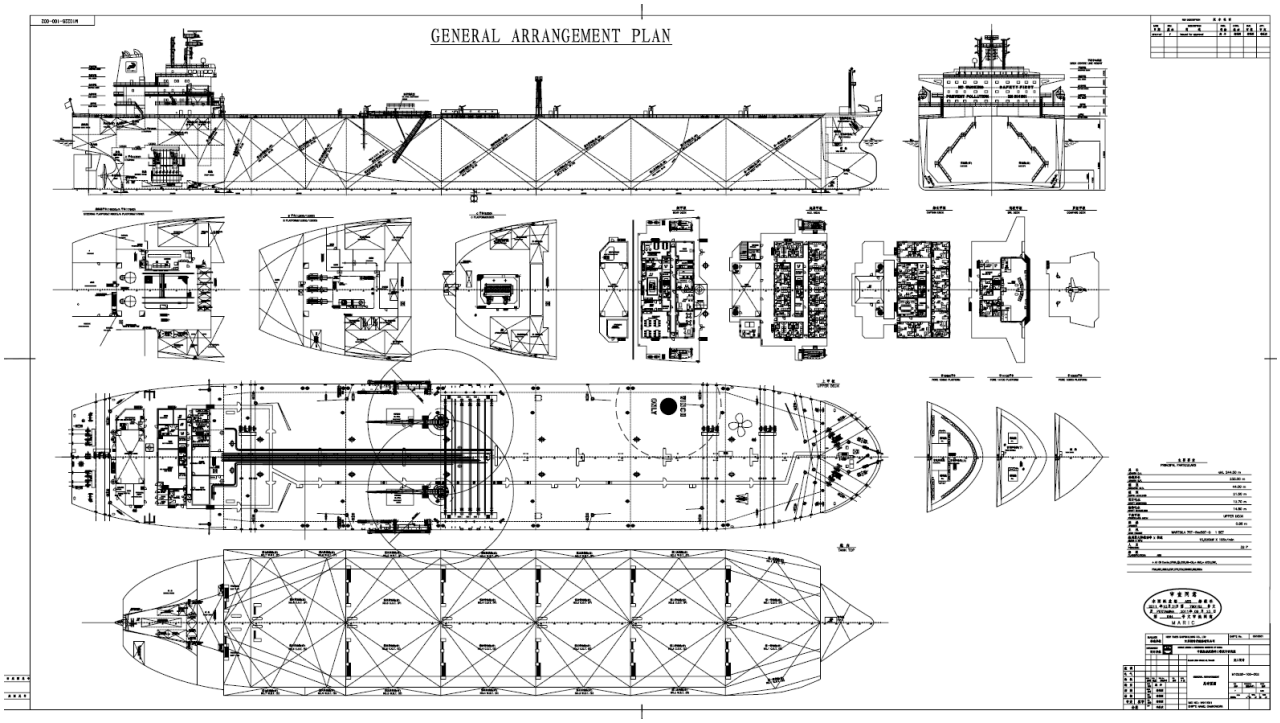

Figure 2. General Arrangement FSO Gamkonora

Figure 3 below is the result of FSO Gamkonora modeling on Vessel modeling software:

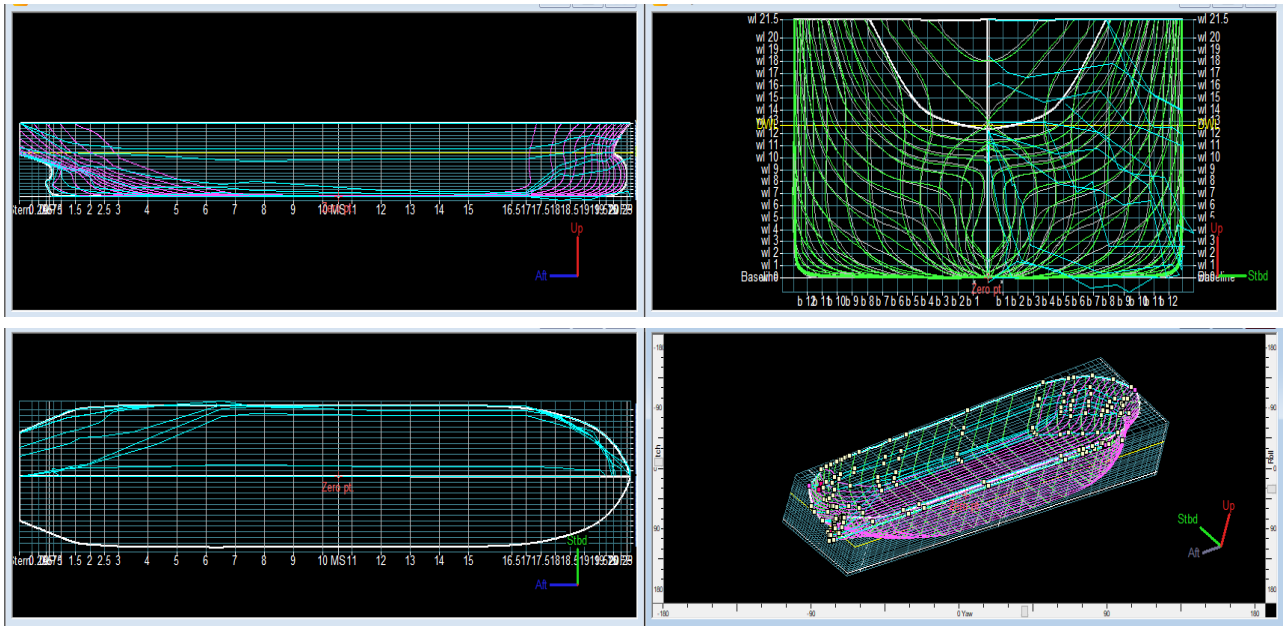

Figure 3. Modeling FSO Gamkonora using Vessel Modeling Software

B. FSO Hydrostatic Validation

To obtain accurate Gamkonora FSO modeling results according to the actual situation, the model design must be validated. Model validation was carried out by comparing the data from the hydrostatic calculation results from the Vessel modeling software with the hydrostatic data from FSO Gamkonora contained in the stability booklet. This is intended to review the accuracy of this FSO model so that the feasibility of the model can be known for use in subsequent analyses.

The model validation criteria used refer to [10] with an error in displacement with a maximum value of 2% and for parameters such as longitudinal center of buoyancy, vertical center of buoyancy, longitudinal center of flotation, transverse metacentric height, and longitudinal metacentric height with a maximum value of 1 %.

Table 4 following are the results of modeling validation between the Vessel modeling software model and data on the stability booklet under full load conditions or T = 12.7 m.

TABLE 4.
FSO VALIDATION RESULTS FULL LOAD CONDITION

Parameter	Limit Criteria	Data	Software	Correction Percentage	Status
Displacement	2%	109,431.3 ton	110,182 ton	-0.69%	Pass
VCB	1%	6.64 m	6.657 m	-0.26%	Pass
KMT	1%	19.31 m	19.351 m	-0.21%	Pass
Coefficient Block (CB)	2%	0.818	0.802	1.96%	Pass
Coefficient Prismatic (CP)	2%	0.821	0.817	0.49%	Pass
Coefficient Midship (CM)	2%	0.996	0.994	0.20%	Pass
Coefficient Waterline (CW)	2%	0.912	0.898	1.54%	Pass

While the Table 5 following are the result of modeling validation between the Vessel modeling software model and the data in the stability booklet under light load conditions or T = 4.2 m.

TABLE 5.
FSO VALIDATION RESULTS LIGHT LOAD CONDITION

Parameter	Limit Criteria	Data	Software	Correction Percentage	Status
Displacement	2%	32,627.6 ton	32,749 ton	-0.4%	Pass
VCB	1%	2.2 m	2.21 m	-0.4%	Pass
KMT	1%	38.04 m	38.43 m	-1.0%	Pass
Coefficient Block (CB)	2%	0.736	0.726	1.4%	Pass
Coefficient Prismatic (CP)	2%	0.745	0.760	-2.0%	Pass
Coefficient Midship (CM)	2%	0.9882	0.985	0.3%	Pass
Coefficient Waterline (CW)	2%	0.798	0.811	-1.6%	Pass

Criteria based on the errors contained in the table above which have values below the validation criteria mentioned by IACS, it can be concluded that the Vessel modeling software model meets and is suitable for use in subsequent analyses.

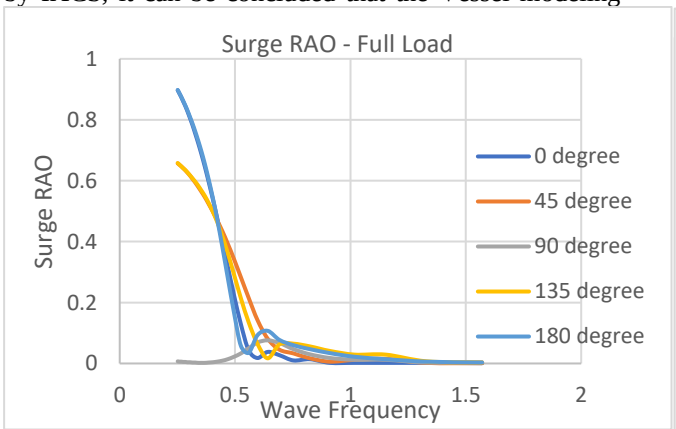

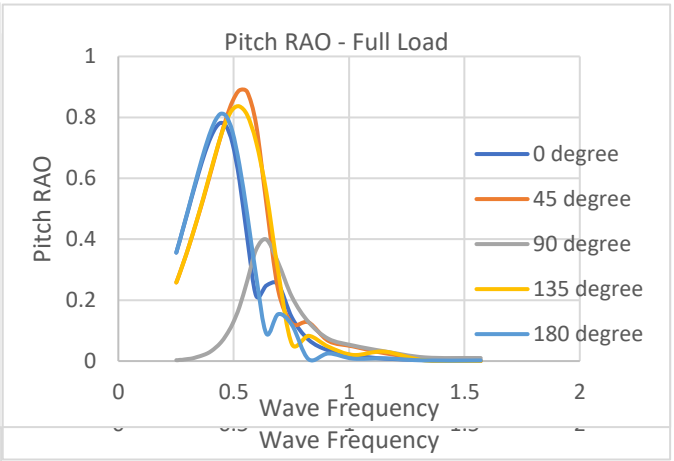

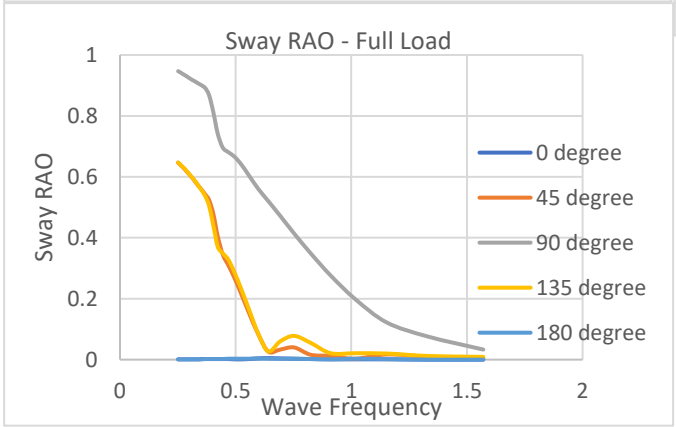

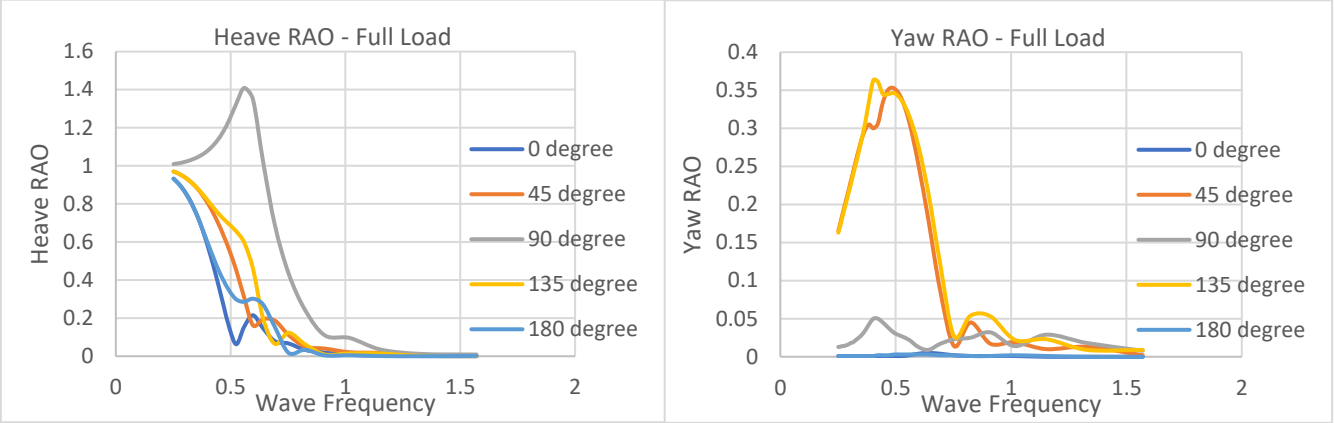

Figure 4. RAO FSO Free Floating Condition (Full Load)

C. Response Amplitudo Operator (RAO) Analysis

Based on the Figure 4 above, the FSO motion characteristics in free floating conditions with full load loading conditions produce RAO graphs for each heading direction. The highest response for translational surge motion is 0.898 m/m at heading 180°, sway is 0.947 m/m at heading 90°, and heave is 1.409 m/m at heading 90°. While the highest response for rotational movement, roll motion is 3.463 deg/m at heading 90°, pitch is 0.889 deg/m at heading 45°, and yaw is 0.363 deg/m at heading 135°.

D. FSO Modeling on Dynamic Analysis Software

The FSO modeling that will be analyzed refers to the geometry of the ship structure in accordance with the General Arrangement, namely MT Gamkonora. FSO modeling in Dynamic analysis software is carried out by incorporating hydrodynamic behavior from Vessel modeling software dynamic analysis results and other parameters. Figure 5 is the geometry of the FSO structure modeling on Dynamic analysis software.

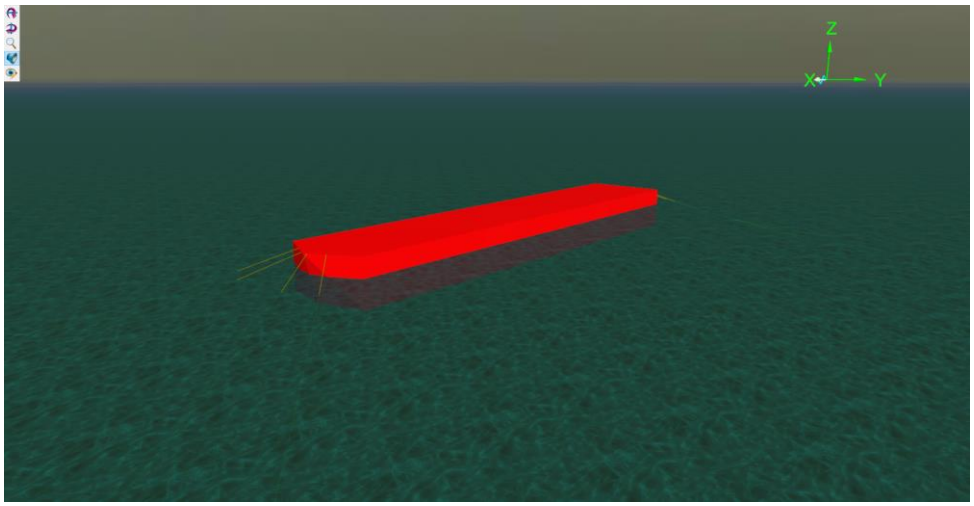

Figure 5. FSO Structural Geometry Modeling on Dynamic Analysis Software

After FSO modeling carried out on Dynamic analysis software, the mooring chain was also modeled using the data in the Table 6 as follows:

TABLE 6.
MOORING CHAIN DIMENSION DATA

Type	Chain, Studlink	
Grade	R4	
Length	345	m
Diameter	87	mm
Minimum Breaking Load	7,682	kN

The FSO mooring configuration modeling and environmental load heading directions on Dynamic analysis software are as shown in Figure 6 and 7 below.

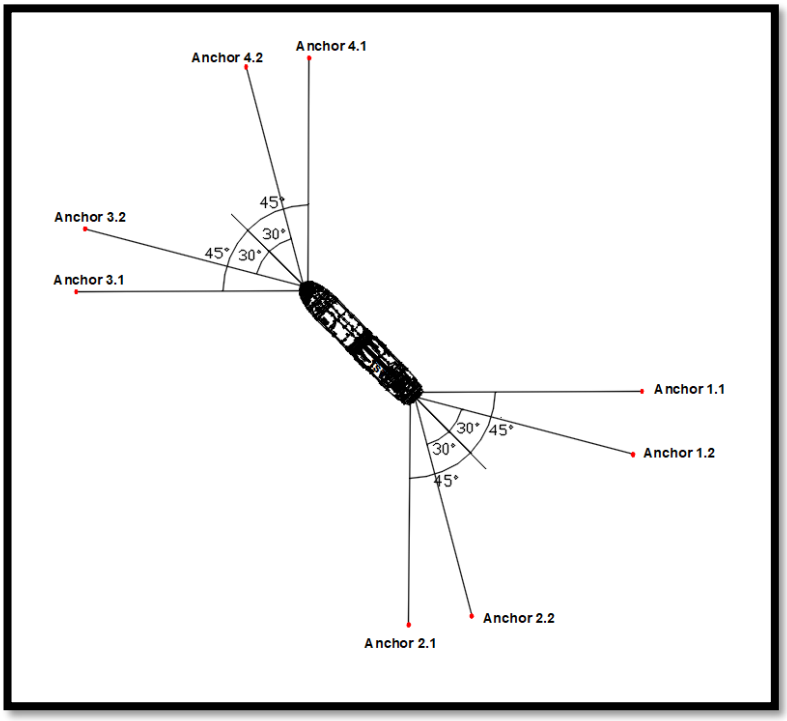

Figure 6. FSO Mooring Line Configuration Modeling on Dynamic Analysis Software

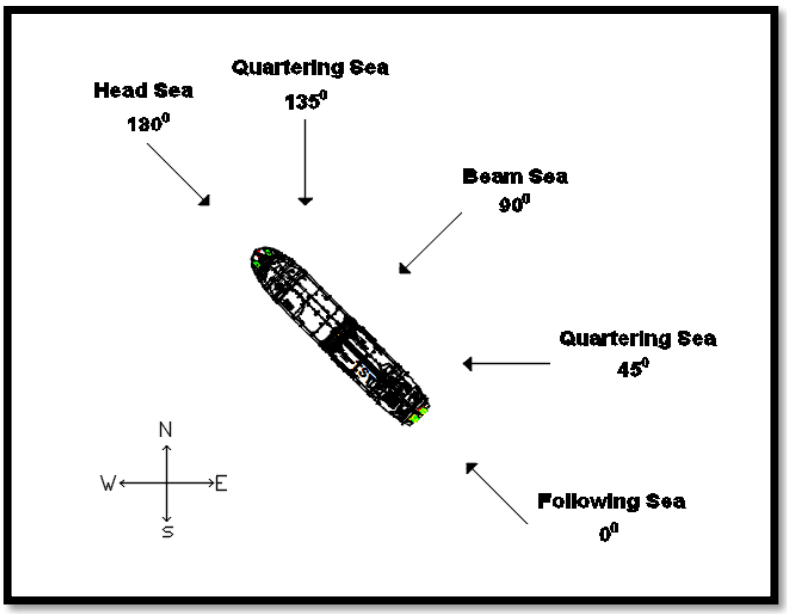

Figure 7. Modeling the Environmental Load Heading Direction on Dynamic Analysis Software

Water depth data in this study is 34 meters. While the environmental data used in this analysis is 1 yearly data or operating conditions. Environmental data and wave scatter data are presented in Table 7 and 8 below:

TABLE 7.
OPERATING ENVIRONMENT DATA

Return Period (years)	Hs (m)	Tp (s)	Wind (m/s)	Current (m/s)
1	2.0	7.1	9.9	0.7

TABLE 8.
WAVE SCATTER DATA

Individual Wave Height (m)	Significant Wave Height (m)	Wave Peak Period (s)	Number of Occurrence	Probability Occurrence
H	**Hs**	**Tp**		**Pi**
0.00-0.25	0.25	2.74	3,590.50	40.94%
0.25-0.50	0.50	3.87	2,922.80	33.33%
0.50-0.75	0.75	4.74	1,300.20	14.83%
0.75-1.00	1.00	5.48	547.60	6.24%
1.00-1.25	1.25	6.12	232.60	2.65%
1.25-1.50	1.50	6.71	99.80	1.14%
1.50-1.75	1.75	7.25	43.00	0.49%
1.75-2.00	2.00	7.75	18.70	0.21%
2.00-2.25	2.25	8.22	8.20	0.09%
2.25-2.50	2.50	8.66	3.70	0.04%
2.50-2.75	2.75	9.08	1.80	0.02%
2.75-3.00	3.00	9.49	0.70	0.01%
3.00-3.25	3.25	9.87	0.30	0.00%
3.25-3.50	3.50	10.25	0.10	0.00%
3.50-3.75	3.75	10.61	0.10	0.00%
			8,770.10	**100.0000%**

The wave scatter data based on the above is summarized into 6 significant wave height classes as shown in Table 9.

TABLE 9.
SUMMARY OF WAVE SCATTER DATA

Individual Wave Height (m)	Significant Wave Height (m)	Wave Peak Period (s)	Number of Occurrence	Probability Occurrence
H	Hs	Tp		Pi
0.00-0.50	0.50	3.87	6,513.30	74.27%
0.50-1.00	1.00	5.48	1,847.80	21.07%
1.00-1.50	1.50	6.71	332.40	3.79%
1.50-2.00	2.00	7.75	61.70	0.70%
2.00-2.50	2.50	8.66	11.90	0.14%
2.50-3.75	2.75	9.08	3.00	0.03%
			8,770.10	100.0000%

E. Corrosion Influence Analysis Scenario

The scenarios that will be analyzed in this research are variations in corrosion, variations in significant wave heights and peak periods, as well as variations in the direction of environmental loading. Based on these variations, the scenarios to be analyzed are 120 load cases. The following are the variations used in the analysis of the effects of corrosion:

1) The Direction of Environmental Loads

The environmental load direction scenarios used in this research are 5 directions given in Table 10 the below:

TABLE 10.
ENVIRONMENTAL LOAD HEADING DIRECTION SCENARIO

Environmental Heading
0°
45°
90°
135°
180°

2) Significant Wave Heights and Peak Periods

The scenario of significant wave height and peak period is obtained from the wave scatter data which is divided into 6 classes as shown in the Table 11 below:

TABLE 11.
SCENARIO OF SIGNIFICANT WAVE HEIGHT AND PEAK PERIOD

Hs	Tp
0.50 m	3.87 s
1.00 m	5.48 s
1.50 m	6.71 s
2.00 m	7.75 s
2.50 m	8.66 s
2.75 m	9.08 s

3) Corrosion and Anchor Chain Diameter
Scenarios of the influence of the corrosion rate are indicated by the large diameter of the anchor chain. The effect of corrosion used in this research is 4 variations according to the Table 12:

TABLE 12.
SCENARIO EFFECT OF CORROSION & ANCHOR CHAIN DIAMETER

Corrosion	Diameter
0%	87 mm
5%	82.65 mm
10%	78.3 mm
15%	73.95 mm

F. Anchor Chain Tension Analysis Effect of Corrosion

FSO mooring tension analysis in this study used the Dynamic analysis software. The analysis was carried out using the Time-Domain method, each of which was simulated using the cut-off method for 20 minutes (1200 seconds). The analysis is carried out on a Time-Domain basis because the factors contained therein are non-linear which are irrelevant if done with the Frequency-Domain. Therefore, to accommodate these non-linear factors, the equations of motion from Newton's 2nd law are solved in terms of time functions. The approach taken in this method uses a time integration procedure and generates a time history response based on the time function x(t).

There are 24 scenarios of the spread mooring system with variations in Hs and the effects of corrosion, where in each scenario the environmental loads are 0º, 45º, 90º, 135º and 180º. In each direction of loading, an analysis was carried out under ULS conditions. Tension that has been obtained on each mooring line, then the safety factor is checked according to API RP 2 SK to find out if the mooring line is still within safe limits or not (ULS > 1.67 and ALS >1.25). The results of the largest tension values in 24 scenarios are as shown in Table 13 below:

TABLE 13.
RESULT OF MAXIMUM EFFECTIVE TENSION ON ANCHOR CHAIN EFFECT OF CORROSION

		Hs					
		0.5 m	1.0 m	1.5 m	2.0 m	2.5 m	2.75 m
Corrosion 0%	Max Tension	1,007.22	1,031.91	1,095.56	1,163.38	1,482.88	1,695.14
	Line	Chain 4.1	Chain 4.1	Chain 4.1	Chain 4.1	Chain 4.1	Chain 4.1
	Env. Heading	90°	90°	90°	90°	90°	90°
Corrosion 5%	Max Tension	933.53	957.54	1,001.15	1,091.83	1,447.43	1,666.12
	Line	Chain 4.1	Chain 4.1	Chain 4.1	Chain 4.1	Chain 4.1	Chain 4.1
	Env. Heading	90°	90°	90°	90°	90°	90°
Corrosion 10%	Max Tension	863.68	885.52	934.22	995.96	1,359.52	1,643.20
	Line	Chain 4.1	Chain 4.1	Chain 4.1	Chain 4.1	Chain 4.1	Chain 4.1
	Env. Heading	90°	90°	90°	90°	90°	90°
Corrosion 15%	Max Tension	798.00	814.33	858.01	962.31	1,173.72	1,625.48
	Line	Chain 4.1	Chain 4.1	Chain 4.1	Chain 4.1	Chain 4.1	Chain 4.1
	Env. Heading	90°	90°	90°	90°	90°	90°

G. Fatigue Analysis

In the results of the analysis of the anchor chain tension due to corrosion, the time history recording of the effective tension was obtained. Time history recording data is divided into 3 segments (Figure 8), namely:

1. *Splash zone*
The area where the anchor chain periodically enters and exits the water when the unit is at its operating depth. In general, this zone is between 5 m above and 4 m below the water level.
2. *Mid-catenary zone*
The anchor chain area is below the splash zone and always above the touch down zone.
3. *Touch down zone*
The area where the chain starts to touch the sea bed to the anchor.

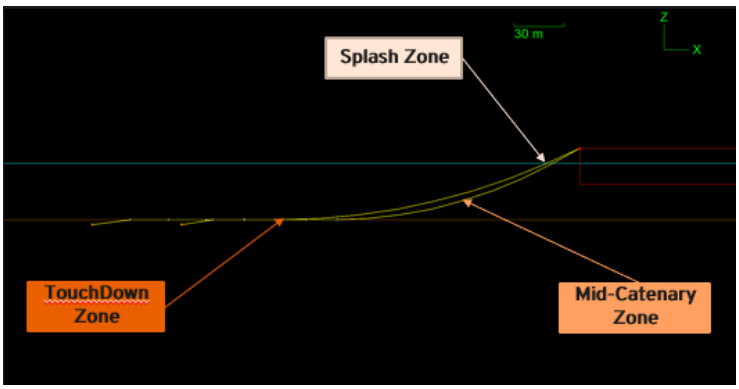

Figure 8. Division of 3 Segment Zones

Using the help of Dynamic analysis software software with the fatigue analysis module and precipitation calculation method, the time history effective stress data is calculated for the values of the stress ranges and the number of cycles for each stress range into a histogram as shown in Figure 9 below.

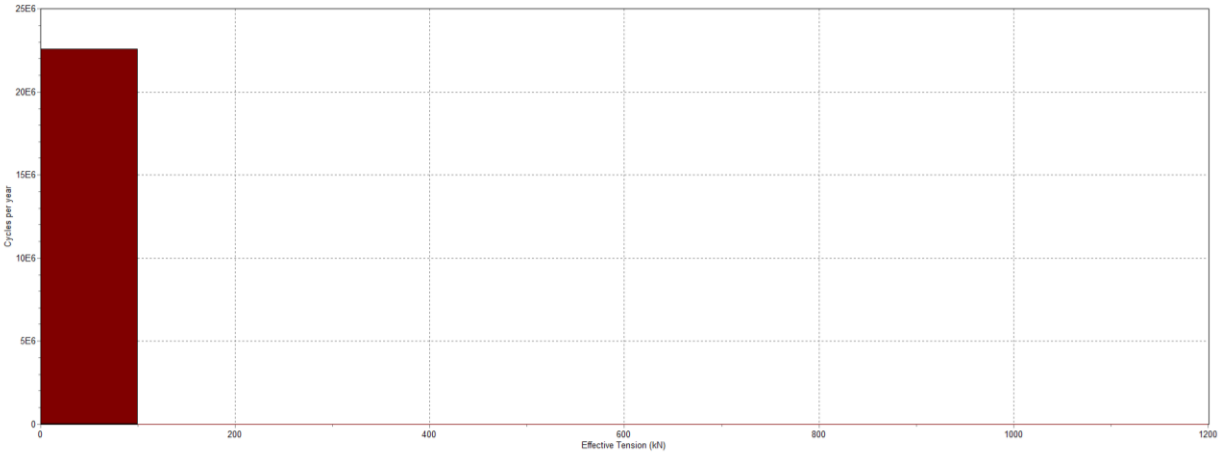

Figure 9. Example of a Rainflow Counting Effective Tension Histogram

From the histogram of the rainflow counting calculation above, the total results for the value of the voltage range and the number of cycles for each Hs variation are as shown in Table 14:

TABLE 14.
TENSION RANGE AND NUMBER OF CYCLES THAT OCCUR EACH SIGNIFICANT WAVE HEIGHT

Tension Range (kN)	Significant Wave Height					
	0.5 m	1.0 m	1.5 m	2.0 m	2.5 m	2.75 m
100	21,661,537.23	17,393,337.83	15,498,746.09	18,227,842.97	18,345,229.08	11,784,646.51
200	0.00	0.00	144,725.26	236,896.15	118,497.89	39,593.69
300	0.00	0.00	0.00	157,930.77	118,497.89	131,978.98
400	0.00	0.00	0.00	0.00	43,888.11	65,989.49
500	0.00	0.00	0.00	0.00	87,776.22	92,385.29
600	0.00	0.00	0.00	0.00	48,276.92	26,395.80
700	0.00	0.00	0.00	0.00	30,721.68	127,573.49
800	0.00	0.00	0.00	0.00	26,332.86	21,990.31
900	0.00	0.00	0.00	0.00	0.00	48,404.67
1000	0.00	0.00	0.00	0.00	0.00	8,792.41
1100	0.00	0.00	0.00	0.00	0.00	4,405.49

However, because the probability of each variation in significant wave height coming is not the same in the real world, the number of cycles must be adjusted to the wave scatter or the probability of significant wave height coming to the sea location used in the analysis. By combining the number of cycles for each voltage range with probability, the cycle values are obtained which have been adjusted according to the wave scatter in Table 15 as follows.

TABLE 15.
PROBABILITY WAVE SCATTER WAVE AT PAPA TERMINAL

Hs	Probability
0.50	0.7427
1.00	0.2107
1.50	0.0379
2.00	0.0070
2.50	0.0014
2.75	0.0003

Thus, Table 16 below is a table of voltage range cycles that have been adjusted to the probability obtained from the wave scatter data presented in the table above.

TABLE 16.
PROBABILITY ADJUSTED TENSION RANGE CYCLE

Tension Range (kN)	Significant Wave Height						Total
	0.5 m	1.0 m	1.5 m	2.0 m	2.5 m	2.75 m	
100	16,087,398.14	3,664,657.15	587,425.82	128,237.75	24,892.33	4,031.19	20,496,642.38
200	0.00	0.00	5,485.31	1,666.63	160.79	13.54	7,326.26
300	0.00	0.00	0.00	1,111.09	160.79	45.15	1,317.02
400	0.00	0.00	0.00	0.00	59.55	22.57	82.12
500	0.00	0.00	0.00	0.00	119.10	31.60	150.70
600	0.00	0.00	0.00	0.00	65.51	9.03	74.54
700	0.00	0.00	0.00	0.00	41.69	43.64	85.32
800	0.00	0.00	0.00	0.00	35.73	7.52	43.25
900	0.00	0.00	0.00	0.00	0.00	16.56	16.56
1000	0.00	0.00	0.00	0.00	0.00	3.01	3.01
1100	0.00	0.00	0.00	0.00	0.00	1.51	1.51

H. Fatigue Life Analysis

Before calculating the fatigue life, the first thing that must be prepared is the TN-Curve value of the chain being analyzed because the fatigue life calculation uses the Palmgren-Miner rule. The following is the TN-Curve mooring line stud chain based on API RP 2SK [15] used in this calculation.

TABLE 17.
M AND K VALUES ON THE TN-CURVE

Component	*M*	*K*
Common studlink	3.00	1,000
Common studless link	3.00	316
Baldt and Kenter connecting link	3.00	178
Six/multi strand rope	4.09	$10^{(3.20-2.79L_m)}$
Spiral strand rope	5.05	$10^{(3.25-3.43L_m)}$

The Table 17 above is obtained from the following TN-Curves in Figure 10 below.

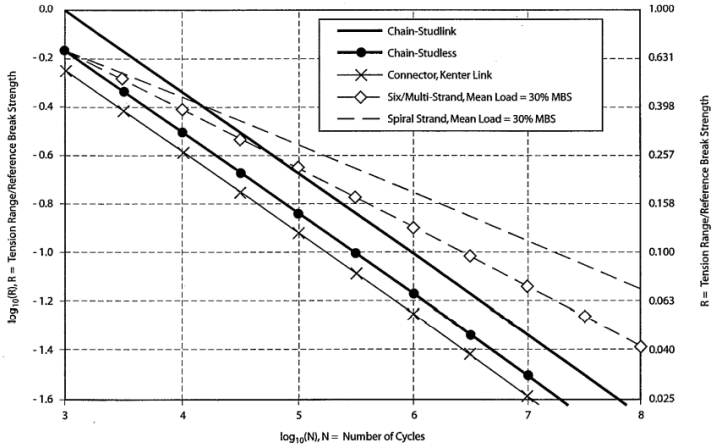

Figure 10. TN-Curves

By applying the number of cycles that occur over a year, the fatigue damage obtained is in the form of annual damage, so that the fatigue life reached by the anchor chain can be calculated with the influence of the corrosion level. From the fatigue damage value, the cumulative damage value is obtained which is used to determine the fatigue life of the anchor chain structure as shown in this Table 18:

TABLE 18.
CALCULATION OF FATIGUE DAMAGE VALUE AND FATIGUE LIFE

Tension Range (kN)	n	K	M	R	R^M	N	Di
100	20,496,642.38	1000	3	0.013017	2.20586E-06	4.53E+08	0.045212635
200	7,326.26	1000	3	0.026035	1.76468E-05	56667352	0.000129285
300	1,317.02	1000	3	0.039052	5.95581E-05	16790327	7.84392E-05
400	82.12	1000	3	0.05207	0.000141175	7083419	1.15939E-05
500	150.70	1000	3	0.065087	0.000275732	3626711	4.1554E-05
600	74.54	1000	3	0.078105	0.000476465	2098791	3.55135E-05
700	85.32	1000	3	0.091122	0.000756608	1321688	6.45576E-05
800	43.25	1000	3	0.10414	0.001129398	885427.4	4.88497E-05
900	16.56	1000	3	0.117157	0.001608069	621863.9	2.66262E-05
1000	3.01	1000	3	0.130174	0.002205856	453338.8	6.6344E-06
1100	1.51	1000	3	0.143192	0.002935994	340600.2	4.42451E-06
					Cumulative Damage		0.045660113
					Fatigue Life (Tahun)		21.90095323

The calculation table above is used to calculate the fatigue life of each anchor chain segment. Thus, fatigue life can be calculated for each anchor chain segment at each corrosion level and summarized in Table 19 below:

TABLE 19.
SUMMARY OF CUMULATIVE DAMAGE VALUE AND FATIGUE LIFE

Corrosion	Segment	Cumulative Damage	Fatigue Life
Corrosion 0%	Splash	0.0457	21.90
	Mid-Catenary	0.0395	25.31
	Touch Down	0.0419	23.85
Corrosion 5%	Splash	0.0466	21.47
	Mid-Catenary	0.0403	24.83
	Touch Down	0.0431	23.22
Corrosion 10%	Splash	0.0483	20.68
	Mid-Catenary	0.0412	24.30
	Touch Down	0.0448	22.35
Corrosion 15%	Splash	0.0702	14.25
	Mid-Catenary	0.0540	18.51
	Touch Down	0.0693	14.42

From the calculation of the fatigue life of the structure, the table above shows that the anchor chain structure has a value of D < 1 so that the structure can be said to be safe for use in operating conditions with the smallest fatigue life of 14.25 years at a corrosion rate of 15%. However, it is known that the fatigue life value does not meet the safety factor criteria in API RP 2SK [15], which is at least 3 times the design life of the anchor chain. The results of the summary of the fatigue life in the table are made into a comparison diagram of the fatigue life of each variation in the degree of corrosion of the anchor chain shown in Figure 11 as follows:

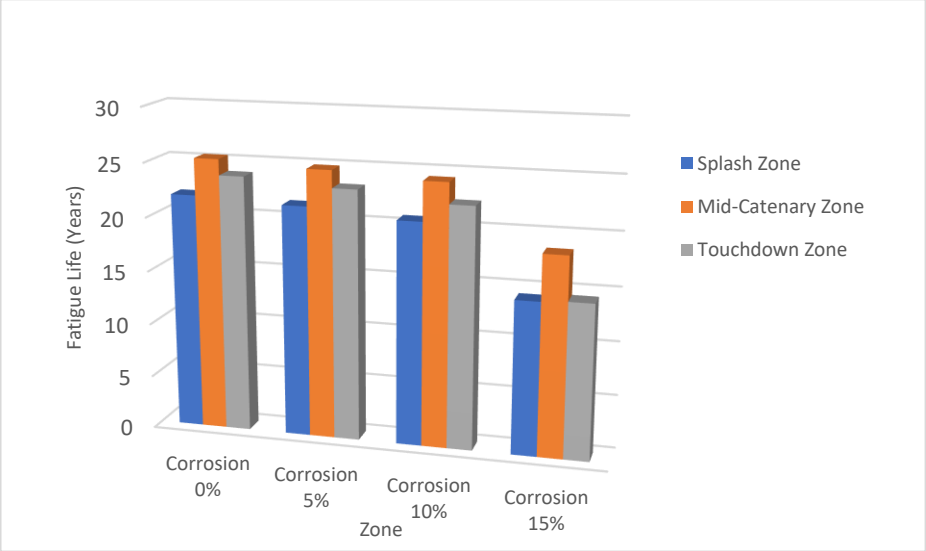

Figure 11. Comparison Chart of Fatigue Life for Each Corrosion Level

IV. CONCLUSION

From the calculations and discussions that have been carried out in CHAPTER IV, several conclusions can be drawn which will also answer the problems that exist in this study. The following are conclusions that can be summarized from this study:

1) The FSO motion characteristics produce varying values in free floating conditions with full load loading conditions. The highest responses for translational and rotational movements are as follows:
   - *surge* value of 0.898 m/m at *heading* 180°,
   - *sway* value of 0.947 m/m at *heading* 90°,
   - *heave* value of 1.409 m/m at *heading* 90°,
   - *roll* value of 3.463 deg/m at *heading* 90°,
   - *pitch* value of 0.889 deg/m at *heading* 45°, and
   - *yaw* value of 0.363 deg/m at *heading* 135°.
2) The greatest stress due to the effect of corrosion on the FSO anchor chain is:
   - 1695,14 kN at 0% corrosion;
   - 1666,12 kN at 5% corrosion;
   - 1643,20 kN at 10% corrosion; and
   - 1625,48 kN at 15% corrosion.

   The maximum stress value occurs in chain 4.1 with the loading direction at 90° and a significant height of 2.75 m. From the results of the analysis of mooring chain tension carried out using the time domain method, it shows that the greatest stress value occurs at each significant wave height variation, each direction of environmental load, and each corrosion effect on each anchor chain that meets the safety factor criteria in API RP 2SK (2005) with no less than a safety factor value of 1,67.
3) 3) From the results of the calculation of the fatigue life of the structure, the results show that the anchor chain structure has D < 1 so that the structure can be

said to be safe for carrying out the mooring process with the smallest structural fatigue life:

- 21,90 years for 0% corrosion;
- 21,47 years for 5% corrosion;
- 20,68 years for 10% corrosion; and
- 14,25 years for 15% corrosion.

However, the smallest fatigue life that has been obtained does not meet the safety factor criteria in API RP 2SK (2005), namely a minimum fatigue life of at least 3 times the design life of the anchor chain.

Based on the results of this study, there are several suggestions that can be made for the development of further research, as follows:

1) Based on the conclusion, it is known that the smallest fatigue life value does not meet the safety factor criteria in API RP 2SK (2005), which is at least 3 times the design life of the anchor chain. Thus, it is necessary to calculate the fatigue life with a larger anchor chain diameter in order to meet the safety factor criteria.
2) It is advisable to carry out fatigue life analysis of the spread mooring system under the influence of corrosion by other methods recommended by the codes, such as simplified fatigue analysis, combined spectrum, spectral fatigue analysis, etc. This aims to determine the comparison of fatigue life values from other methods.
3) It is recommended to perform local strength and fatigue life analysis on the FSO chain stopper on a spread mooring system. This aims to determine the level of security on the mooring line which has an important role in maintaining the FSO movement in carrying out its operations.

REFERENCES

[1] E. B. Djatmiko, "Perilaku dan Operabilitas Bangunan Laut di Atas Gelombang Acak," 2012, pp. 1–27.
[2] S. Junianto, Mukhtasor, R. W. Prastianto, and W. Wardhana, "Motion Responses Analysis for Tidal Current Energy Platform: Quad-Spar and Catamaran Types," China Ocean Eng., vol. 34, no. 5, pp. 677–687, 2020.
[3] K-T. Ma, "Mooring System Engineering for Offshore Structures," In European University Institute, Issue 2, Gulf Professional Publishing, 2018.
[4] J. J. Soedjono, "Diktat Mata Kuliah Kontruksi Bangunan Laut II," Jurusan Teknik Kelautan ITS, 1998.
[5] J. J. Soedjono, "Kuliah Perencanaan Sistem Bangunan Laut I," Jurusan Teknik Kelautan ITS, 1989.
[6] E. B. Djatmiko, "Seakeeping: Perilaku Bangunan Apung di Atas Gelombang," ITS Press, 2003.
[7] Y. Wu, T. Wang, O. Eide, and K. Haverty, "Governing factor and locations of fatigue damage on mooring lines of floating structures," Ocean Engineering, vol. 96, pp. 109-124, 2015.
[8] C. Kang, C. Lee, S. H. Jun, and Y. T. Oh, "Fatigue analysis of spread mooring line," Int. J. Environ. Chem. Geol. Geophys. Eng., vol. 10, no. 5, 2016.
[9] R. W. Prastianto, Ramzi, and Murdjito, "Mooring Analysis of SPAR Type Floating Offshore Wind Turbine in Operation Condition due to Heave, Roll, and Pitch Motions," IOP Conference Series: Earth and Environmental Science, IOP Publishing, 2019.
[10] IACS, "L5 Computer Software for Onboard Stability Calculations," pp. 1–12, 2017.
[11] ABS, "Rules for Building and Classing Mobile Offshore Drilling Units," Houston: American Bureau of Shipping, 2018.
[12] S. K. Chakrabarti, S. K., "Hydrodynamics of Offshore Structures," In European University Institute (Issue 2), Mid-County Press, 1987.
[13] N. M. Sabana, E. B. Djatmiko, and R. W. Prastianto, "Fatigue Life of Mooring Lines on External Turret Floating LNG for Different Pretension and Water Depth," IPTEK The Journal for Technology and Science, vol. 30(1), April, 2019.
[14] DNVGL-OS-E301, "Position Mooring." July. 114, 2015.
[15] API RP 2SK, "Recommended Practice for Design and Analysis of Station Keeping Systems for Floating Structures," 2005.
[16] S. Junianto, Mukhtasor, R. W. Prastianto, and C. H. Jo, "Effects of demi-hull separation ratios on motion responses of tidal current turbines-loaded catamaran," Ocean Syst. Eng., vol. 10, no. 1, pp. 87–110, 2020.
[17] A. H. Adaalah, R. W. Prastianto, Murdjito, F. Syalsabila, and M. R. Syarifudin, "Analysis of Mooring Line Tension in Floating Collar Net Cage,", 6th International Conference on Marine Technology (SENTA 2021), IOP Publishing, 2022.
[18] BKI, "Guidelines for Floating Production Installations," vol. 3, 2013.
[19] G. Alencar, "A user-friendly tool for fatigue assessment of steel structures according to Eurocode 3. New Trends on Integrity, Reliability and Failure," July, pp. 1–9, 2016.
[20] DKPU ITS, "Zulu Terminal Marine Conceptual Study," Project Report, 2023.